Distinct step-like changes in G values for the losses of typical functional groups in poly(ethylene terephthalate) along boron ion tracks around the detection threshold

Yamauchi, Tomoya ; Kusumoto, Tamon ; Ueno, Takuya ; Mori, Yutaka ; Kanasaki, Masato ; Oda, Keiji ; Kodaira, Satoshi ; Barilion, Remi

(Citation)
Radiation Measurements,116:51-54

(Issue Date)
2018-09

(Resource Type)
journal article

(Version)
Accepted Manuscript

(URL)
https://hdl.handle.net/20.500.14094/90005197

Distinct step-like changes in G values for the losses of typical functional groups in poly(ethylene terephthalate) along boron ion tracks around the detection threshold

Tomoya Yamauchi*[a], Tamon Kusumoto[a,c], Takuya Ueno[a], Yutaka Mori[a], Masato Kanasaki[a], Keiji Oda[a], Satoshi Kodaira[b], Rémi Barillon[c],

[a] *Graduate School of Maritime Sciences, Kobe University, 5-1-1 Fukaeminami-machi, Higashinada-ku, 658-0022 Kobe, Japan*

[b] *Radiation Measurement Research Team, National Institute of Radiological Sciences, National Institutes for Quantum and Radiological Science and Technology, 4-9-1 Anagawa, Inage-ku, 263-8555 Chiba, Japan*

[c] *Institute Pluridisiplinaire Hubert Curien, 23 rue du Loess, 67037 Strasbourg Cedex 2, France*

G values of the losses of typical functional groups in PET films along boron ion tracks have been determined using FT-IR spectrometry. G value for the loss of aromatic-ring clearly increases above 270 eV/nm. Those of ester and ethylene increase around the slightly lower stopping power of 250 eV/nm. The detection thresholds are defined by determining the original points from which the evolution of etch pit starts along the latent track, when the chemical etching was progressing starting from the front surface of each incident ion trajectory. The thresholds for B, C, N, O, Ar and Kr ions have been determined for other kind of PET sheets. Values of the sensitivity at the thresholds are fairly higher at heavy ions with smaller atomic number.

Keyword : PET; Ion tracks; threshold; G value

*Corresponding author

Phone: +81-78-431-6307

Fax: +81-78-431-6355

e-mail: yamauchi@maritime.kobe-u.ac.jp (Tomoya Yamauchi)

1. Introduction

Poly(ethylene terephthalate), PET, has been recognized as an etched track detector with relatively high detection thresholds depending on the industrial products (Bhattacharyya et al., 2016; Drach et al., 1987; Somogyi et al., 1976). Stacked PET detectors with different kinds of detectors of poly(allyl diglycol carbonate), PADC, and polyimide (Kapton) have made it possible to identify the nuclear charge of heavy ions from the intense laser plasma in complex radiation fields (Nishiuchi et al., 2015). In the nuclear nano pore membranes, PET has been utilized as a base material (Apel, 2001; Siwy et al., 2003). Sub-nanometer pores in PET produced by UV exposure following heavy ions irradiation found to have high selectivity for alkali and alkaline earth metal ions (Wen et al., 2016).

In order to control the response as an etched track detector or the pore size in membrane materials, fundamental studies on the latent track structure should be inevitable. Many FT-IR spectral examinations have been performed for ion tracks in PET by several authors (Biswas et al., 1999; Liu et al., 2000; Steckenreiter et al., 1997, Zue et al., 2002). In our last study on the tracks in PET, we found the clearly different dependence of chemical damage parameters, like G values, between He and C ions on the stopping power around the detection threshold (Yamauchi et al., 2012). In this study, modified track structure along boron ions (B-10 and B-11) has been examined. Through comprehensive etching tests, the detection thresholds for heavy ions are also determined.

2. Experiments and the definition of detection threshold

PET films with a thickness of 2.5 μm (Goodfellow, ES301025) were used to assess the G value. B ion irradiations (B-10 and B-11 ions with 6 MeV/u) were made at the medium energy irradiation room of Heavy Ion Medical Accelerator in CHIBA (HIMAC), on the stacked 50 films in which the ions stopped completely (Yamauchi et al., 2012). FT-IR measurements were carried out in vacuum both before and after the irradiations using FT/IR-6100S (JASCO, Japan), in which the entire system, including interferometer, photon detector and sample room, can be evacuated.

The etching tests were made for PET sheets with a thickness of 1.0 mm (SUMITOMO, EPG100), in 6 M KOH solution kept at 50ºC. Ion irradiations were carried out at HIMAC, including quasi-relativistic energies for different kinds of ions,

as shown in Fig. 1. The solid circles indicate the etch pit formation. The open ones signify no etch pit. For the purpose of precise discussions, we have applied the rigorous definition on the detection thresholds as shown in Fig. 2. The threshold is defined as the point where the latent track turns to etchable under the normal incidence, which can be identified as the original point of etch pit evolution during chemical etching in this figure. The samples were irradiated as stacked, to work themselves as moderators and to keep the original points under a certain depth from the surface. The etch pits were observed by a scanning electron microscope (Neo Scope, JCM-5000, JEOL), as well as an optical microscope. The stopping powers at the thresholds were calculated using SRIM code (Ziegler, 2004).

3. G values along B ion tracks

Fig. 3 (a). shows the monotonically decreasing behaviors of the relative absorbance of carbonyl (1718 cm^{-1}), A/A_0, which is the ratio of the net absorbance after the irradiation, A, to the original one, A_0, as a function of B-10 ion fluence for three different films of the first, the second and the third from the top surfaces. Fig. 3 (b). shows those of aromatic-ring (1504 cm^{-1}). Except for the data set of aromatic-ring in the first film with 268 eV/nm, trends in each figure are similar to each other. Including the previously reported data for other heavy ions (Yamauchi et al., 2012), the observed trends are expressed well by the following formula against the ion fluence, *F*,

$$A/A_0 = 1 - \sigma_i \cdot F, \quad (1)$$

where σ_i is an experimental constant in units of cm^2. This means the removal cross section in which considered bonds were lost. The effective track core radius, r_t, was obtained from this ($\sigma_i = \pi r_t^2$). When the overlapping of tracks was negligible, the relative absorbance is equivalent to the survival fraction of considered bonds, N/N_0, that is the ratio of the number density of the considered bond after the irradiation, N, to that of original one, N_0. G-values were calculated using the following formula:

$$G = \frac{\sigma N_0}{\left(\overline{-dE/dx}\right)}, \quad (2)$$

where $\left(\overline{-dE/dx}\right)$ is the average stopping power in each film (Mori et al., 2011; Kusumoto et al., 2016). As shown in Fig. 4 (a), distinct step-like changes are observed at the stopping power of 250 eV/nm in G values for the loss of carbonyl. We have observed the similar changes in G values for the losses of ethylene, as well as C-O-C

which composes ester, at the identical stopping power. On the other hand, the step-like changes for the loss of aromatic-ring are observed at the higher value of 270 eV/nm, as indicated in Fig. 4 (b). Return to the experimental results, the removal cross section of carbonyl in the first film is identical to those in the other films (Fig. 3. (a)), but that of aromatic-ring in the first is clearly small compared to the others (Fig. 3. (b)).

As discussed in the previous work, the effective track core radius increase rapidly at the step from 0.16 nm to 0.5 nm (Yamauchi et al., 2012). With decreasing B ions energies, the discontinuous slight damage turned to be significant rapidly above 270 eV/nm, covering one repeat unit of PET in track radial direction. Carbonyl, Aromatic-ring and CH_2 were clearly damaged only above the same stopping power. We have proposed a model to describe sudden increase of radiation damage that the breakings at the two most neighbor esters could be resulted in the significant losses of these functional groups (Yamauchi et al., 2012). Effects of low energy electrons around ion track have never examined well (Fromm et al., 2015). In order to evaluate structure of secondary elections, we have started a simulation using a Monte Caro Code of Geant4-DNA tool kits (Kusumoto et al., 2017).

4. Detection thresholds for each ion

Fig. 5. shows the evolutions of the pit radii, r, of indicating heavy ions as a function of the thickness of layer removed, h. The plotted points are the averages over more than 50 measurements for etch pits. Each solid line were obtained by the least square fitting. As shown in this figure, the extrapolated fitting lines do not pass through the origin. The coordinates of the intersections should represent the beginning of etch pits in PET, where etch pits start their own evolution. From the slope of the fitted line, $\beta = dr/dh$, the reduced etch rate ratio, S, was evaluated using the following formula (Somogyi, 1980; Yamauchi et al., 1992),

$$S = \left(1+\beta^2\right)/\left(1-\beta^2\right) - 1. \qquad (3)$$

Fig. 6. indicates the obtained sensitivity at each threshold, as a function of the stopping power. The sensitivity decreases with increasing ion's nuclear charge. Similar dependence was also observed for polyimide (Kapton), including U ions (Yamauchi et al. 2013&2015). It is difficult to give some identical physical parameters for the detection threshold, because the sensitivity is clearly different among these ion species.

5. Conclusion

A series of FT-IR studies has been made for B ion irradiated PET films. The G value for the loss of aromatic-ring increased above 270 eV/nm. Those of ester and ethylene increased above 250 eV/nm. Ester is the most radiosensitive part in PET, aromatic-ring and ethylene should be lost when adjacent two ester on both sides were destroyed. The detection thresholds for B, C, N, O, Ar and Kr ions have been determined by etching tests against the different kind of PET sheets. The threshold in the stopping power increased with increasing the ion's nuclear charge. The sensitivity at the thresholds decreased with increasing the ion's nuclear charge. New approaches should be started to explain the feature of the detection thresholds in PET, including the microscopic structure of secondary electrons around latent tracks.

Acknowledgements

We express our thanks to the staff of NIRS-HIMAC for their support during the experiment (H138). This work was made as a part of the Research Project with Heavy Ions at NIRS-HIMAC. This work was supported by JSPS KAKENHI Grant Number 16K05002.

References

Apel, P., 2001. Track etching technique in membrane technology. *Radiat. Meas.* 34, 559-566.

Bhattacharyya, R., Dey, S., Ghosh, S. K., Maulik, A., Raha, S., Syam, D., 2016. Deyermination of the detection threshold for polyethylene terephthalate (PET) nuclear track detector (NTD). *Nucl. Instrum. Meth. B.* 370, 63-66.

Biswas, B., Lotha, S., Fink, D., Singh, J.P., Avasthi, D.K., Yadav, B.K., Bose, S.K., Khating, D.T., Avasthi, A.M., 1999, The effects of swift heavy ion irradiation on the radiochemistry and melting characteristics of PET. *Nucl. Instrum. Meth. B.* 159, 40-51.

Drach, J., Price, P.B., Salamon, M.H., 1987. Characteristics of Corona polyethylene

terephthalate track detectors. *Nucl. Instrum. Meth. B.* 28, 49-52.

Fromm, M., Quinto, M.A., Weck, P. F., Chanpion, C., 2015, Low energy electrons and swift ion track structure in PADC. Radiat. Phys. Chem. 115, 36-42.

Kusumoto, T., Mori, Y., Kanasaki, M., Ikenaga, R., Oda, K., Kodaira, S., Kitamura, H., Barillon, R., Yamauchi, T., 2016. Radiation chemical yields for losses of typical functional group in PADC films for high energy protons registered as unetchable tracks. *Radiat. Meas.* 87, 35-42.

Kusumoto. T., Bitar, Z. EL., Okada, S., Gillet P., Arbor, N., Kanasaki, M., Oda, K., Nourredine, A.M., Kurashige, H., Barillon, R., Yamauchi, T., 2017. Radial electron fluence around ion tracks as a new physical parameter for the detection threshold of PADC using Geant4-DNA toolkit. International Conference on Nuclear Tracks and Radiation Measurements, 28th August – 1st September, Strasbourg, France.

Liu, C., Jin, Y., Zhu, Z., Sun, Y., Hou, M., Wang, Z., Wang, Y., Zhang, C., Chen, X., Liu, J., Li, B., 2000. Molecular conformation changes of PET films under high-energy Ar ion bombardent. *Nucl. Instrum. Meth. B.* 169, 72-77.

Mori, Y., Yamauchi, T., Kanasaki, M., Maeda, Y., Oda, K., Kodaira, S., Konishi, T., Yasuda, N., Barillon, R., 2011. Radiation chemical yields for loss of ether and carbonate ester bonds in PADC films exposed to proton and heavy ion beams. *Radiat. Meas.* 46, 1147-1153.

Nishiuchi, M., Sakaki, H., Esirkepov, T.Zh., Nishio, K., Pikuz, T.A., Faenov, A.Ya., Skobelev, I.Yu., Orlandi, R., Sako, H., Pirozhkov, A.S., Matsukawa, K., Sagisaka, A., Ogura, K., Kanasaki, M., Kiriyama, H., Fukuda, Koura, H., Y., Kando. M., Yamauchi, T., Watanabe, Y., Bulanov, S.V., Kondo, K., Imai, K., Nagamiya, S., 2015. Acceleration of highly charged GeV Fe ions from a low-Z substrate by intense femtosecond laser. *Phys. Plasmas* 22, 033107, 1-8.

Siwy, Z., Apel, P., Dobrev, D., Neumann, R., Spohr, R., Trautmann, C., Voss, K., 2003.

Ion transport through asymmetric nanopores prepared by ion track etching. *Nucl. Instrum. Meth. B.* 208, 143-148.

Somogyi, G., Grabish, K., Scherzer, R., Enge, W., 1976. Revision of the concept of registration threshold in plastic track detectors. *Nucl. Instrum. Meth*. 134, 129-141.

Somogyi, G., 1980. Development of etched nuclear tracks. *Nucl. Instrum. Meth*. 173, 21-42.

Steckenreiter, T., Balanzat, E., Fuess, H., Trautmann, C., 1997. Chemical modifications of PET induced by swift heavy ions. *Nucl. Instrum. Meth. B.* 131, 159-166.

Wen, Q., Yan, D., Liu, F., Wang, M., Ling, Y., Wang, P., Kluth, P., Schauries, C., Trautmann, C., Apel., P., Guo, W., Xiao, G., Liu, J., Xue J., Wang, Y., 2016. Highly selective ionic transport through subnanometer pore in polymer films. *Adv. Func. Mater.* 26, 5796-5803.

Yamauchi, T., Matsumoto, Oda, K., Miyake, H., 1995. Missing track segment on the growth curve of etch-pit radius. *Radiat. Meas.* 24, 101-104.

Yamauchi, T., Mori, Y., Morimoto, A., Kanasaki, M., Oda, K., Kodaira, S., Konishi, T., Yasuda, N., Tojo, S., Honda, Y., Barillon, R., 2012. Threshold of etchable track formation and chemicall damage parameters in poly(ethylene terephthalate), bisphenol A polycarbonate, and poly(allyl diglycol carbonate) films at the stopping powers ranging from 10 to 12,000 keV/μm. *Jpn. J. Appl. Phys.* 51, 05631, 1-5.

Yamauchi, T., Matsukawa, K., Mori, Y., Kanasaki, M., Hattori, A., Matai, Y., Kusumoto, T., Tao, A., Oda, K., Kodaira, S., Konishi, T., Kitamura, H., Yasuda, N., Barillon, R., 2013. Applicability of Polyimide Films as Etched-Track Detectors for Ultra-Heavy Cosmic Ray Components. Appl. Phys. Express 6, 046401, 1-4.

Yamauchi, T., Kusumoto, T., Matsukawa, K., Mori, Y., Kanasaki, A., Oda, K., Kodaira, Yoshida, K., Yanagisawa, Y., Kambara, T., Yoshida, A., 2015. Response of polyimide

films to U ion beams as etched-track detectors. RIKEN Accel. Prog. Rep. 48, 254.

Zhu, Z., Liu, C., Sun, Y., Liu, J., Tang, Y., Jin, Y., Du, J., 2002. Modification of polyethylene terephthalate under high-energy heavy ion irradiation. *Nucl. Instrum. Meth. B.* 191, 723-727.

Ziegler, J.F., 2004. SRIM-2003. *Nucl. Instrum. Meth. B.* 219-220, 1027-1036.

Figure captions

Fig. 1. Track registration data for PET plotted on the graph of the electronic stopping power against the normalized ion speed (β =v/c).

Fig. 2. Definition of the detection threshold for track detectors based on the original point for the etch pit evolution.

Fig. 3. Reduction of the relative absorbance of C=O bond (a) and aromatic-ring (b) with the fluence of B-10 ions.

Fig. 4. G values for the losses of C=O (a) and aromatic-ring (b) as a function of the stopping power. Open symbols are cited from the previous study (Yamauchi et al., 2012).

Fig. 5. Etch pit evolution in radii due to chemical etching in 6 M KOH solution kept at 50ºC.

Fig. 6. Sensitivity of heavy ions at each detection threshold in PET.

Fig. 1. Yamauchi et al., Distinct Step-like Changes in G values

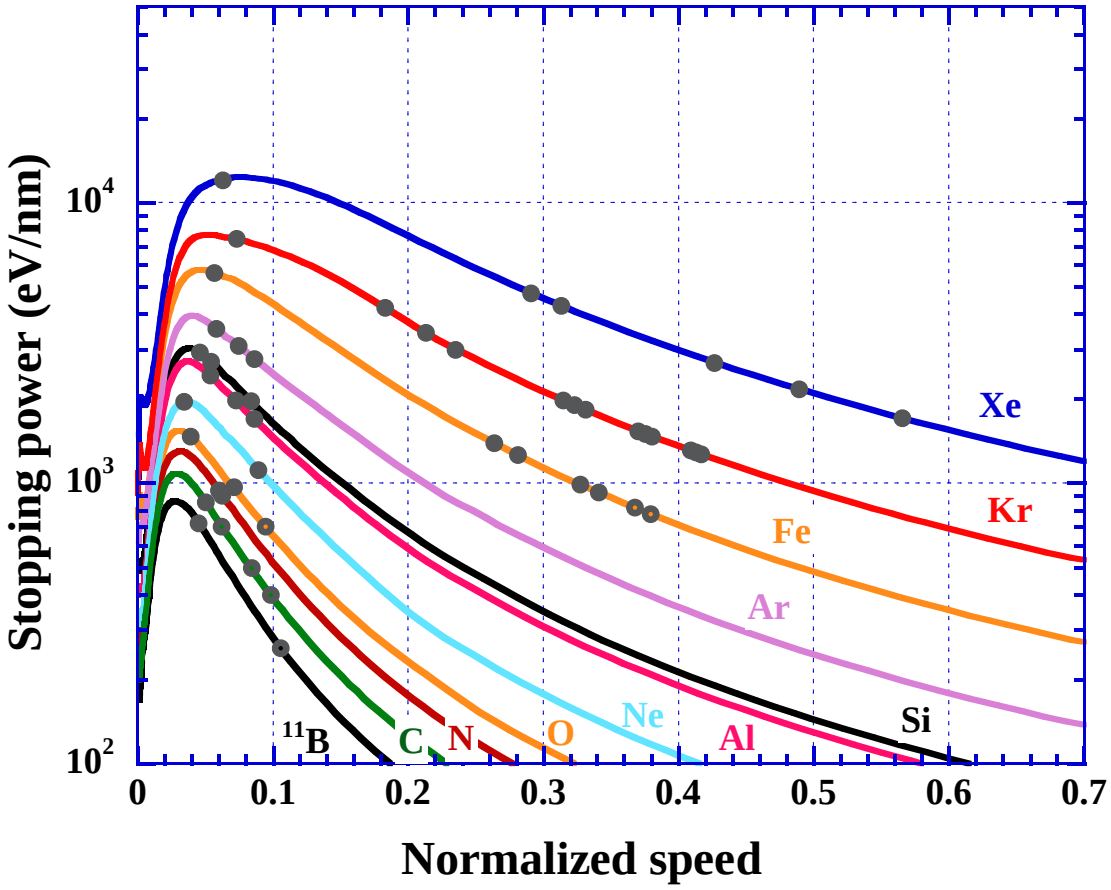

Fig. 2. Yamauchi et al., Distinct Step-like Changes in G values

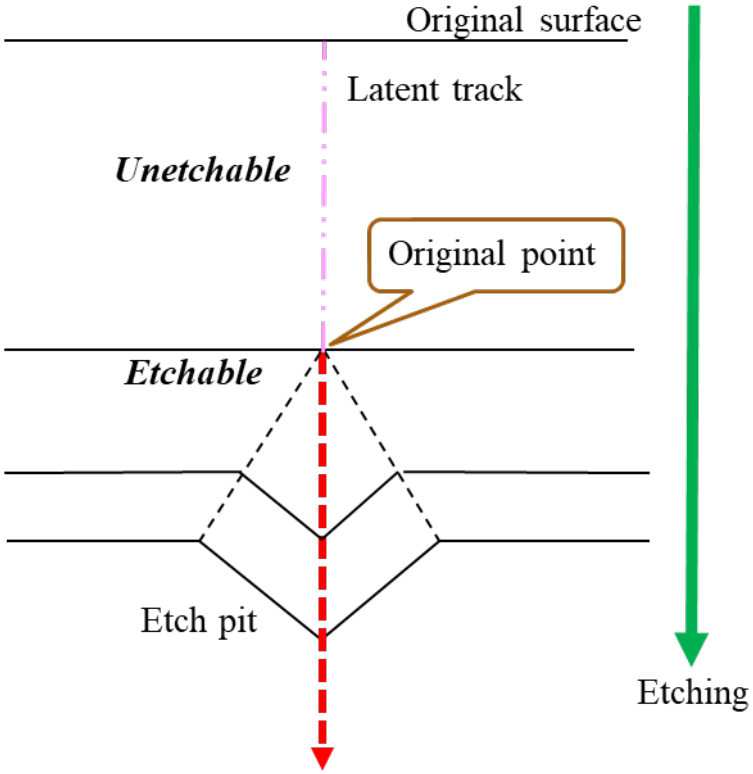

Fig. 3. Yamauchi et al., Distinct Step-like Changes in G values

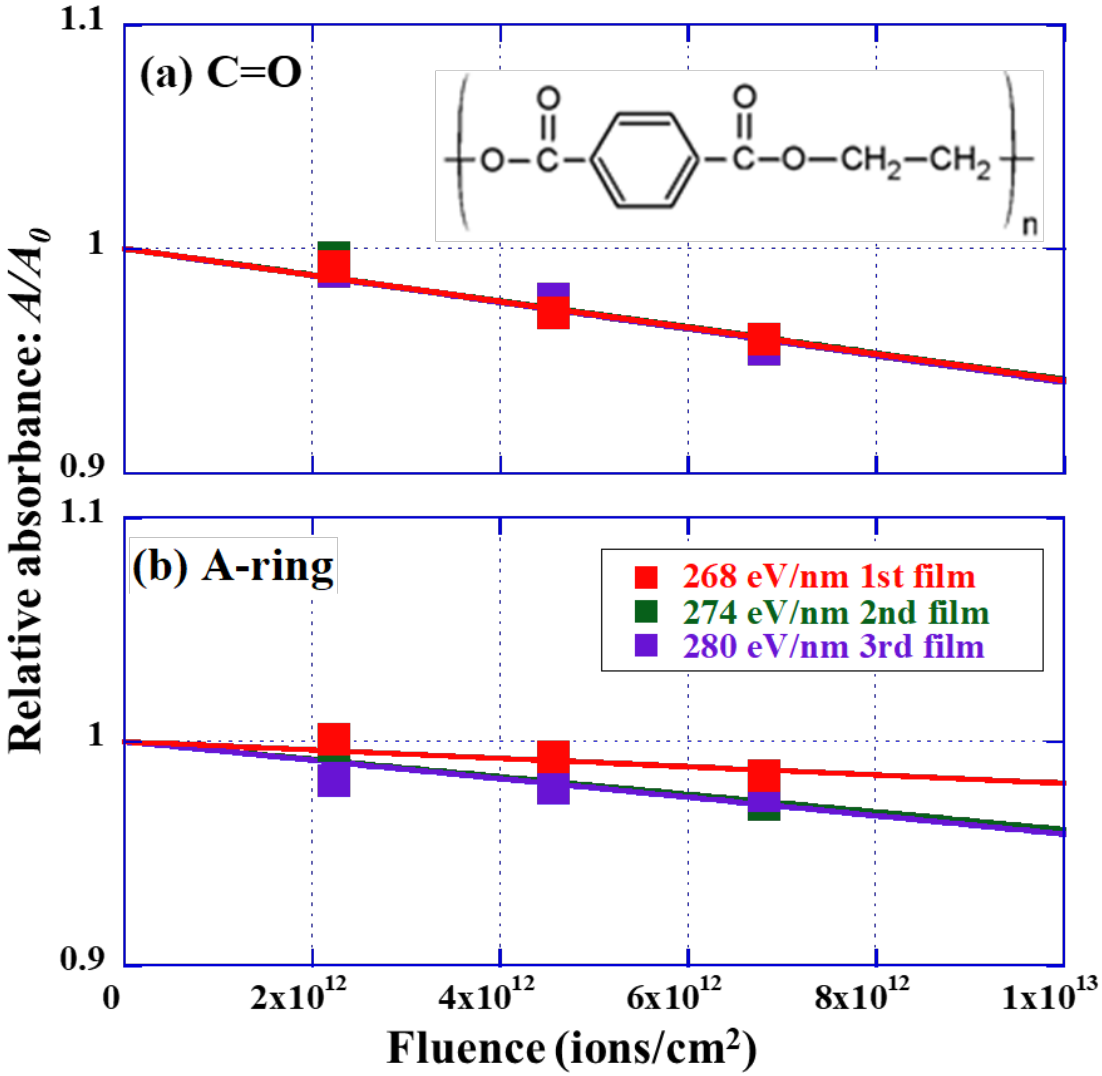

Fig. 4. Yamauchi et al., Distinct Step-like Changes in G values

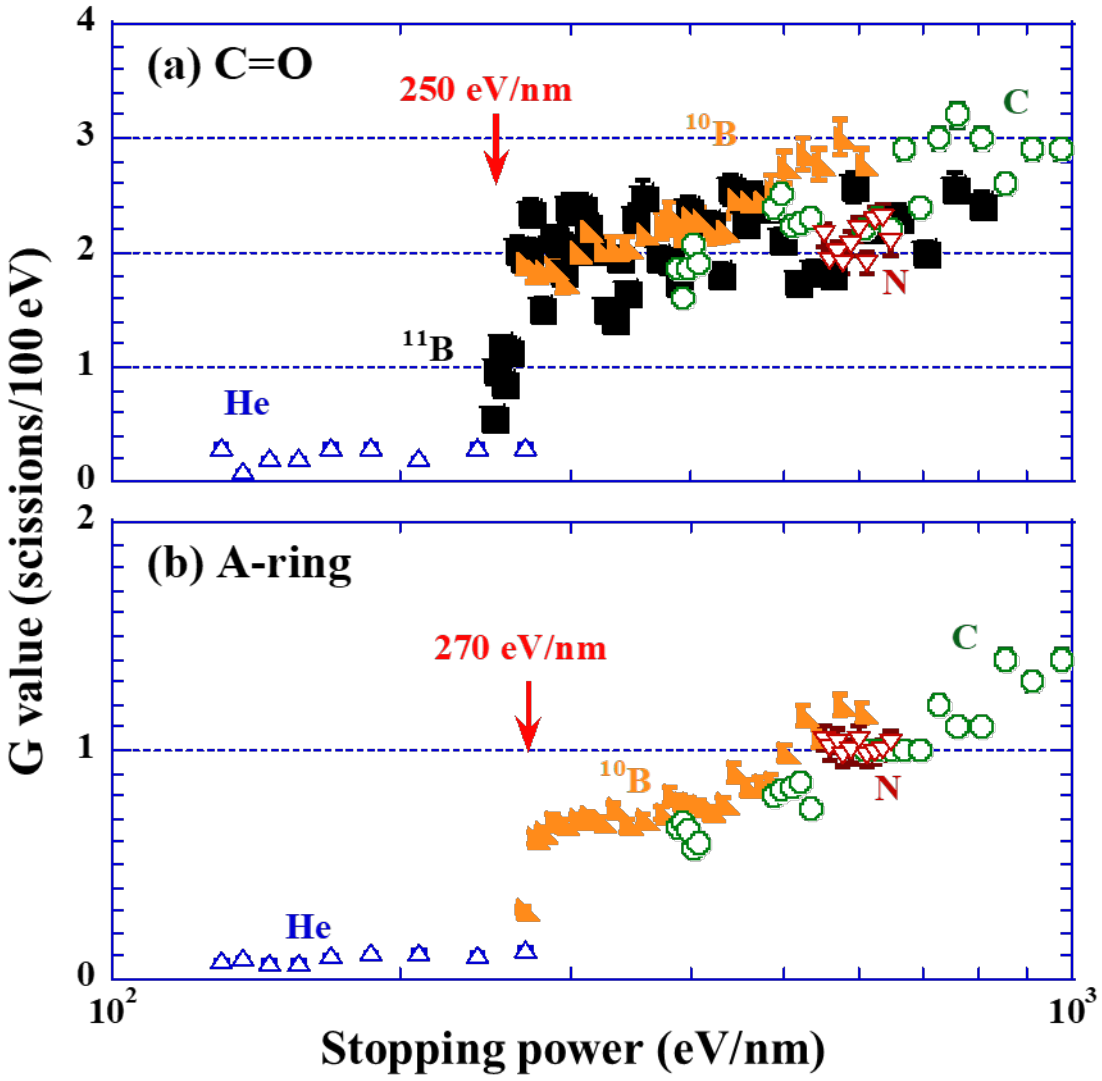

Fig. 5. Yamauchi et al., Distinct Step-like Changes in G values

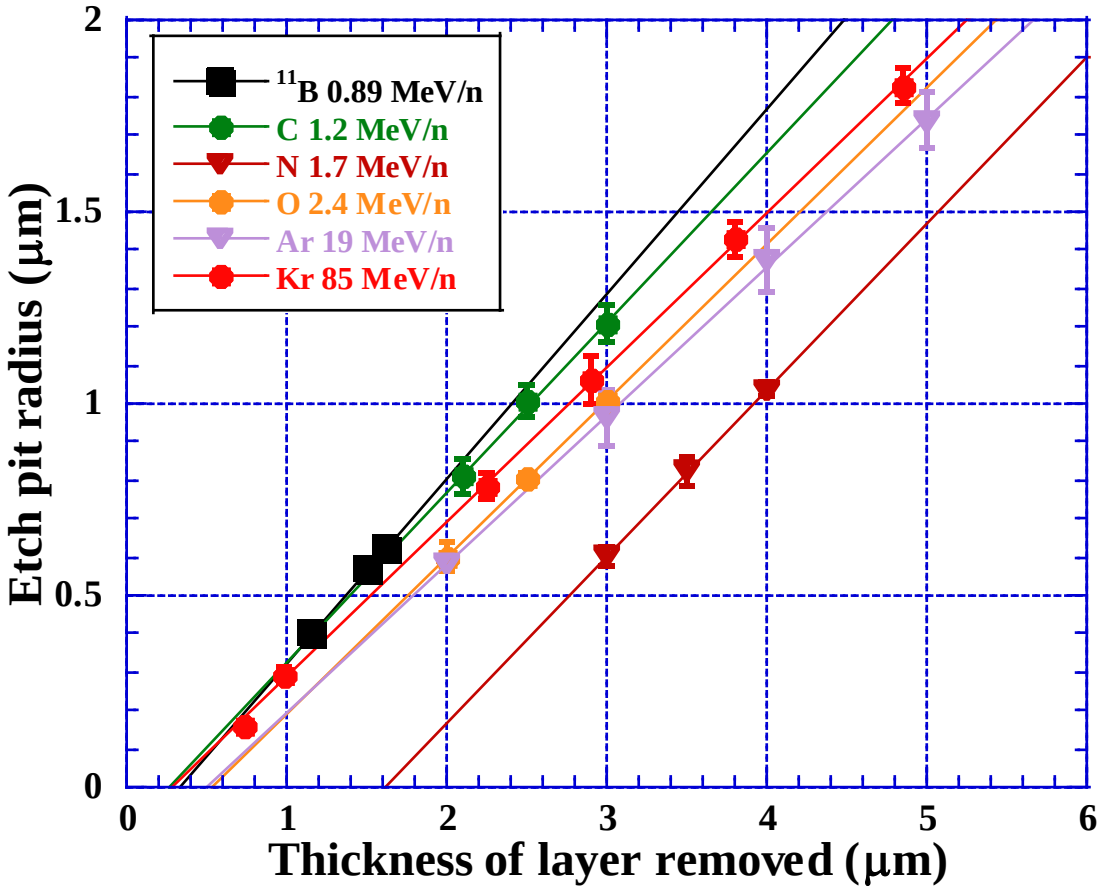

Fig. 6. Yamauchi et al., Distinct Step-like Changes in G values